Structural and Quantum Chemical Study of Bi_5^{3+} and Isoelectronic Main-Group Metal Clusters. The Crystal Structure of Pentabismuth(3+) Tetrachlorogallate(III) Refined from X-ray Powder Diffraction Data and Synthetic Attempts on Its Antimony Analogue

Stefan Ulvenlund,[†] Kenny Ståhl,[‡] and Lars Bengtsson-Kloo*[,§]

Department of Chemistry, Imperial College of Science, Technology and Medicine, South Kensington, London SW7 2AY, England, and Divisions of Inorganic Chemistry 1 and Inorganic Chemistry 2, Department of Chemistry, Lund University, P.O. Box 124, S-221 00 Lund, Sweden

Received December 7, 1994[⊗]

Pentabismuth(3+) tetrachlorogallate(III), $(Bi_5^{3+})(GaCl_4^-)_3$, has been synthesized by reducing a $BiCl_3-GaCl_3$ melt with bismuth metal and the crystal structure refined from X-ray (Cu Kα_1) powder diffraction data. The structure was found to belong to space group *R*-3*c*, with the lattice parameters $a = 11.871(2)$ Å and $c = 30.101(3)$ Å ($Z = 6$). It is isostructural with the previously characterized $Bi_5(AlCl_4)_3$. An attempt to synthesise the antimony analogue $Sb_5(GaCl_4)_3$ by reducing a $SbCl_3-GaCl_3$ mixture with gallium metal produced a black solid phase. The gallium content of this phase is consistent with the stoichiometry $Sb_5(GaCl_4)_3$, and the Raman spectrum of the phase dissolved in $SbCl_3-GaCl_3$ comprises strong, low-frequency bands attributable to Sb−Sb stretch vibrations in Sb_5^{3+} or another reduced antimony species. Quantum chemical analyses have been performed for the isoelectronic, trigonal pyramidal *closo*-clusters Sn_5^{2-}, Sb_5^{3+}, Tl_5^{7-}, Pb_5^{2-}, and Bi_5^{3+}, both with extended Hückel (eH) and Hartree−Fock (HF) methods. The HF calculations were performed with and without corrections for the local electron−electron correlation using second-order Møller−Plesset perturbation theory (MP2). All theoretical results are compared and evaluted with respect to experimental cluster structures and vibrational frequencies. The results from the calculations agree well with available experimental data for the solid-state structures and vibrational spectra of these cluster ions, except for the Tl_5^{7-} ion. Isolated Tl_5^{7-} is suggested to be electronically unstable because of the high charge density. The Sb_5^{3+} cluster ion is indicated to be stable. According to the calculations, Sn_5^{2-} and Pb_5^{2-} may be described in terms of edge-localized bonds without substantial electron density between the equatorial atoms, whereas Sb_5^{3+} and Bi_5^{3+} have electron density evenly distributed over all M−M vectors. Furthermore, the theoretical results give no support for a $D_{3h} \rightarrow C_{4v}$ fluxionality of these clusters.

Introduction

Naked main-group metal clusters, of which the isoelectronic species Sn_5^{2-}, Tl_5^{7-}, Pb_5^{2-}, and Bi_5^{3+} are typical examples, constitute a large and growing class of metal−metal bonded species on which a substantial amount of solid-state data have been accumulated in the literature.[1−4] Considering the number of such species isolated in the solid state, there is a definite paucity of data regarding their solution chemistry as well as their spectroscopic properties. No doubt, this paucity is to a large extent caused by the extreme air and moisture sensitivity of these ions and of the solvents necessary to stabilize them. In the case of the M_5^y clusters, Sn_5^{2-}, Tl_5^{7-}, Pb_5^{2-}, and Bi_5^{3+} have all been structurally characterized in the solid state,[5−7] but only Bi_5^{3+} seems to have been detected in solution and investigated by spectroscopic methods.[8−11] The extremely high charge density of Tl_5^{7-} (present in $Na_2K_2Tl_{19}$)[5] probably disqualifies it from being stable in solution, but no obvious reason for an inherent instability of Sn_5^{2-} and Pb_5^{2-} in solution exists. However, in contrast to the $Pb_xSn_{9-x}^{4-}$ clusters ($x = 0-9$) and Sn_4^{2-}, which have all been thoroughly investigated in solution by means of UV/vis[12] and $^{207}Pb/^{119}Sn$ NMR spectroscopy,[12−17] spectroscopic data on M_5^{2-} have never been reported and the difficulties of detecting these clusters in solution have been discussed.[15] Nevertheless, Sn_5^{2-} and Pb_5^{2-} clusters have been proposed to be fluxional in solution on the basis of the NMR experiments on the $Pb_xSn_{9-x}^{4-}$ ($x = 0-9$, all fluxional in solution) and Sn_4^{2-} systems.[12]

Several solid compounds containing naked, cationic bismuth clusters (Bi_5^{3+}, Bi_8^{2+}, and Bi_9^{5+}) have been synthesized either by molten salt routes[2] or by using so-called superacid systems.[1] Bi_5^{3+} has been synthesized by both these routes. Reduction of a molten 1:3 mixture of $BiCl_3$ and $AlCl_3$ with a stoichiometric

[†] Imperial College of Science.
[‡] Division of Inorganic Chemistry 2, Department of Chemistry, Lund University.
[§] Division of Inorganic Chemistry 1, Department of Chemistry, Lund University.
[⊗] Abstract published in *Advance ACS Abstracts,* November 15, 1995.

(1) Gillespie, R. J.; Passmore, J. *Adv. Inorg. Chem. Radiochem.* **1975**, *17*, 49.
(2) Corbett, J. D. *Prog. Inorg. Chem.* **1976**, *21*, 129.
(3) Gillespie, R. J. *Chem. Soc. Rev.* **1979**, *8*, 315.
(4) Corbett, J. D. *Chem. Rev.* **1985**, *85*, 383.
(5) Dong, Z.; Corbett, J. D. *J. Am. Chem. Soc.* **1994**, *116*, 3429.
(6) Edwards, P. A.; Corbett, J. D. *Inorg. Chem.* **1977**, *16*, 903.
(7) Krebs, B.; Mummert, M.; Brendel, C. *J. Less-Common Met.* **1986**, *116*, 159.
(8) Burns, R. C.; Gillespie, R. J.; Luk, W. C. *Inorg. Chem.* **1978**, *17*, 3596.
(9) Bjerrum, N. J.; Boston, C. R.; Smith, G. P. *Inorg. Chem.* **1967**, *6*, 1162.
(10) Bjerrum, N. J.; Davis, H. L.; Smith. G. P. *Inorg. Chem.* **1967**, *6*, 1603.
(11) Bjerrum, N. J.; Smith, G. P. *Inorg. Chem.* **1967**, *6*, 1968.
(12) Wilson, W. L. Thesis, The University of Michigan, 1982.
(13) Rudolph, R. W.; Wilson, W. L.; Parker, F.; Taylor, R. C.; Young, D. C. *J. Am. Chem. Soc.* **1978**, *100*, 4629.
(14) Pons, B. S.; Santure, D. J.; Taylor, R. C.; Rudolph, R. W. *Electrochim. Acta* **1981**, *26*, 365.
(15) Rudolph, R. W.; Wilson, W. L.; Taylor, R. C. *J. Am. Chem. Soc.* **1981**, *103*, 2480.
(16) Wilson, W. L.; Rudolph, R. W.; Lohr, L. L.; Taylor, R. C.; Pyykkö, P. *Inorg. Chem.* **1986**, *25*, 1535.
(17) Rothman, M. J.; Bartell, L. S.; Lohr, L. L. *J. Am. Chem. Soc.* **1981**, *103*, 2482.
(18) Corbett, J. D. *Inorg. Chem.* **1968**, *7*, 198.

0020-1669/96/1335-0223$12.00/0

amount of bismuth metal yields $Bi_5(AlCl_4)_3$,[7,18] whereas oxidation of bismuth metal by AsF_5 in SO_2 solution yields $Bi_5(AsF_6)_3 \cdot 2SO_2$.[8]

With this background, it is quite puzzling that data on Sb_5^{3+} and other cationic antimony clusters are very scarce. Paul *et al*. have reported that the oxidation of antimony metal in $S_2O_8F_2-HSO_3F$ mixtures produces highly colored solutions, the UV/vis spectra of which were first attributed to Sb_4^{2+} and Sb_8^{2+}.[19] However, these spectra were later reinterpreted as being due to the formation of cationic sulfur clusters formed in the reduction of S(VI) by antimony metal.[1] More consistent is the claim that the oxidation of antimony metal in liquid AsF_5 produces a white solid product analyzed as $SbAsF_6$.[20] The diamagnetism of this poorly characterized Sb(I) product led the authors to propose a polymeric, Sb−Sb bonded structure of this alleged Sb(I) compound, rather than the presence of isolated Sb^+ ions. Attempts to synthesize solid compounds containing cationic Sb-clusters in the liquid $Sb-SbX_3$ and $Sb-SbX_3-AlX_3$ systems (X = Cl, Br, I), *i.e*. to parallel the synthesis of cationic Bi-clusters, fail because of the low solubility of antimony metal in these systems.[21−24] However, the presence of Sb_4^{2+} (or rather the molecular Sb_2X_4) in solution has been proposed on the basis of emf,[25] electric conductivity,[26] and vapor pressure measurements[27] on these molten systems. The low solubility of antimony metal in the liquid $SbCl_3-AlCl_3$ system (albeit several orders of magnitude higher than in neat liquid $SbCl_3$)[23] as compared with the bismuth case may tentatively be explained as a consequence of two interacting factors: (1) a weaker reducing capacity of antimony metal as compared to bismuth and (2) a lower thermal stability of antimony clusters than of their bismuth analogues. This would account for the assumption that a metal−metal-bonded Sb(I) compound ($SbAsF_6$ alluded to above) can be synthesized in the strongly oxidizing liquid AsF_5 system at room temperature but not in the high-temperature $Sb-SbCl_3-AlCl_3$ system, which contains the considerably weaker oxidizing agent $SbCl_3$.

Thus, to clarify the questions about the apparent instability of Sn_5^{2-} and Pb_5^{2-} clusters in solution and the enigma of the Sb_5^{3+} ion, we feel that a thorough quantum-chemical study of these clusters is justified. In this respect, we would like to stress that naked main-group clusters are especially optimal systems for a quantum-chemical study. The reasons are two: First, these clusters are only stable under extremely Lewis-acidic (noncoordinating) conditions, and the systems thus are as close to "gas phase" as one can possibly come in condensed phases. Second, the clusters studied here have no unpaired electrons and a large HOMO−LUMO gap, which makes single configurational ground-state calculations unusually good approximations.

Previous theoretical studies of main-group metal M_5^y cluster ions only seem to embrace extended Hückel (eH) calculations[5,18,28−30] and topology.[31] The apparent unwillingness to use more elaborate methods of computation for the analysis of the main-group cluster systems is presumably due to their *deceivingly* simple bonding scheme and the early success in correctly attributing important cluster properties on the basis of very simple bonding models.[18,32] In the eH studies, the bonding has often been claimed to involve p orbitals alone (a claim substantiated by Mössbauer spectroscopy),[33] and because of the large size of these atomic orbitals the contribution from the instantaneous electron−electron correlation has been considered negligible. All M_5^y clusters discussed in this article contain 22 valence (s and p) electrons, of which 10 are occupying the so-called inert electron pairs (nonbonding molecular orbitals) according to the simplified bonding scheme alluded to above. This leaves us with 12 bonding electrons, and the clusters thus obey the Wade−Mingos[34,35] (and Rudolph's PERC)[36] rule ($2n + 2$) for *closo*-clusters. This fact, in turn, means that we should expect a ground-state geometry of D_{3h} (trigonal bipyramidal) symmetry for these clusters, in accordance with what is found experimentally.

We have learned that more accurate calculations and more elaborate bonding models are needed for quantitative or even semiquantitative considerations of linear polyiodide systems.[37] We thus find it appropriate to expose the 12-electron M_5^y *closo*-clusters to a detailed quantum chemical analysis. A proper understanding of the bonding conditions in such clusters is also of vital importance for the understanding of their reaction chemistry, an area which remains almost completely experimentally unexplored.

In this article, we report an *ab initio* theoretical analysis of the M_5^y clusters, as well as the structural characterization of $Bi_5(GaCl_4)_3$ synthesized by the reduction of a $BiCl_3-4GaCl_3$ mixture by bismuth metal. The demonstrated capacity of $GaCl_4^-$ to stabilize cationic clusters, in combination with the low melting points of $GaCl_3$-based systems and the theoretical results for a hypothetical Sb_5^{3+} cluster, leads us to investigate the possibility of synthesizing the antimony analogue $Sb_5(GaCl_4)_3$. The outcome of these attempts is also reported.

Calculations

The extended Hückel (eH) calculations were performed using the CACAO program with the following parameters:[38] Sn($h_{ii}\{5s\} = -16.16$ eV, $\zeta_i\{5s\} = 2.12$, $h_{ii}\{5p\} = -8.32$ eV, $\zeta_i\{5p\} = 1.82$), Sb($h_{ii}\{5s\} = -18.80$ eV, $\zeta_i\{5s\} = 2.32$, $h_{ii}\{5p\} = -11.70$ eV, $\zeta_i\{5p\} = 2.00$), Tl($h_{ii}\{6s\} = -11.60$ eV, $\zeta_i\{6s\} = 2.30$, $h_{ii}\{6p\} = -5.00$ eV, $\zeta_i\{6p\} = 1.60$), Pb($h_{ii}\{6s\} = -15.70$ eV, $\zeta_i\{6s\} = 2.35$, $h_{ii}\{6p\} = -8.00$ eV, $\zeta_i\{6p\} = 2.06$), Bi($h_{ii}\{6s\} = -18.67$ eV, $\zeta_i\{6s\} = 2.56$, $h_{ii}\{6p\} = -7.81$ eV, $\zeta_i\{6p\} = 2.07$).[39,40] The Wolfsberg−Helmholz formula with $K = 1.75$ was used.

Hartree−Fock (HF) calculations with and without corrections according to second-order Møller−Plesset perturbation theory (MP2) for the instantaneous electron−electron correlation were performed using the GAUSSIAN92 program package.[41] In order to indirectly get

(19) Paul, R. C.; Paul, K. K.; Malhotra, K. C. *J. Chem. Soc., Chem. Commun*. **1970**, 453.
(20) Dean, P. A. W.; Gillespie, R. J. *J. Chem. Soc., Chem. Commun*. **1970**, 853.
(21) Corbett, J. D.; Winbush, S.; Albers, F. C. *J. Am. Chem. Soc*. **1957**, *79*, 3020.
(22) Ustinov, A. I.; Petrov, E. S. *Izv. Sib. Otd. Akad. Nauk SSSR, Ser. Khim. Nauk* **1970**, 30.
(23) Sörlie, M.; Smith, G. P. *J. Inorg. Nucl. Chem*. **1981**, *41*, 931.
(24) Dikarev, E. V.; Shevelkov, A. V.; Popovkin, B. A. *Zh. Vses. Khim. Ova. im. D. I. Mendeleeva* **1991**, *36*, 276 (engl transl *Mendeleev Chem. J*. **1991**, *36*, 28).
(25) Corbett, J. D.; Albers, F. C. *J. Am. Chem. Soc*. **1960**, *82*, 533.
(26) Ichikawa, K.; Shimoji, M. *Trans. Faraday Soc*. **1966**, *62*, 3543.
(27) Bruner, B. L.; Corbett, J. D. *J. Inorg. Nucl. Chem*. **1961**, *20*, 62.
(28) Lohr, L. L. *Inorg. Chem*. **1981**, *20*, 4229.
(29) Burns, R. C.; Gillespie, R. J.; Barnes, J. A.; McGlinchey, J. *Inorg. Chem*. **1982**, *21*, 799.
(30) Mingos, D. M. P.; Modrego, J. *New J. Chem*. **1991**, *15*, 9.
(31) King, R. B. *Inorg. Chim. Acta* **1982**, *57*, 79.
(32) Corbett, J. D.; Rundle, R. E. *Inorg. Chem*. **1964**, *3*, 1408.
(33) Rudolph, R. W.; Chowdhry, A. *Inorg. Chem*. **1974**, *13*, 248.
(34) Wade, K. *Adv. Inorg. Chem. Radiochem*. **1976**, *18*, 1.
(35) Mingos, D. M. P. *Acc. Chem. Res*. **1984**, *17*, 311.
(36) Rudolph, W. *Acc. Chem. Res*. **1976**, *9*, 446.
(37) Bengtsson, L. A.; Stegemann, H.; Svensson, P. H. To be published.
(38) Mealli, C.; Proserpio, D. M. *J. Chem. Educ*. **1990**, *67*, 399.
(39) Hoffmann, R.; Bengtsson, L. A. *J. Am. Chem. Soc*. **1993**, *115*, 2666.
(40) Alvarez, S. Unpublished results, 1983.
(41) Frisch, M. J.; Trucks, G. W.; Head-Gordon, M.; Gill, P. M. W.; Wong, M. W.; Foresman, J. B.; Johnson, B. G.; Schlekel, H. B.; Robb, M. A.; Replogle, E. S.; Gomperts, R.; Andres, J. L.; Raghavshari, K.; Binkley, J. S.; Gonzalez, C.; Martin, R. L.; Fox, D. J.; Defrees, D. J.; Baker, J.; Stewart, J. J. P.; Pople, J. A. *Gaussian92*; Gaussian Inc.: Pittsburgh, PA, 1992.

a verification of the proper level of analysis (basis set and correlation), configuration interaction (CISD) calculations were also performed for the M_5^y clusters. The exponents used for d polarization functions were 0.25 for Sn, 0.26 for Sb, 0.15 for Tl, 0.17 for Pb, and 0.17 for Bi. The choice of basis sets is discussed in the Results section.

Throughout this study, experimental data have been used to evaluate the results obtained from the theoretical calculations; *i.e.* the experimentally determined structures, atom−atom distances, and vibrational frequencies serve as the reference state to which all results of the theoretical calculations have been compared.

Experimental Section

Chemicals and General Procedures. All manipulations were performed in a glovebox under dry (<0.3 ppm H_2O) nitrogen. Anhydrous gallium(III) chloride, gallium metal, antimony(III) chloride (all ALFA chemicals, 99.999%), and bismuth metal (Aldrich, 99.999%) were used as received. Bismuth(III) chloride (Aldrich, 98%+) was purified by sublimation, as has previously been described.[42]

Synthesis of $Bi_5(GaCl_4)_3$. $Bi_5(GaCl_4)_3$ was synthesized by reacting a mixture of formal composition $4Bi-BiCl_3-4GaCl_3$ in a Pyrex ampule sealed under vacuum at 300 °C. The reaction mixture was equilibrated for 1 week before being slowly cooled to room temperature. The excess of gallium(III) chloride was removed by sublimation under vacuum at 100 °C. The product is a microcrystalline mass, black in bulk but brick-red when powdered. Microscopic investigation of the powder reveals that the red phase is interspersed by small amounts of one or several other black phases. The same observation has previously been reported for the corresponding $Bi-BiCl_3-AlCl_3$ system and was suggested to be metallic bismuth and/or other reduced bismuth phases (*e.g.* $Bi_8(AlCl_4)_2$).[7,18] Pure, macrocrystalline $Bi_5(AlCl_4)_3$, the synthesis of which is analogous to the one applied here, may be prepared by recrystallization of the crude product from molten $NaAlCl_4$ at 130 °C.[7] However, considering the appreciably higher melting points of the corresponding $MGaCl_4$ salts (M = Na, K, Cs)[43,44] no recrystallization of the present product was attempted. The powder diffraction pattern of the product did not show any reflections other than those of $Bi_5(GaCl_4)_3$. The black phase found is most probably amorphous and is thus less likely to consist of metallic bismuth crystallites acting as growth nuclei for $Bi_5(GaCl_4)_3$, since the high crystal symmetry of bismuth metal results in very strong X-ray reflections even at low concentrations.[45]

$Ga-SbCl_3-GaCl_3$ System. Mixtures of compositions $SbCl_3-4GaCl_3$ and $3Ga-7(SbCl_3-4GaCl_3)$ were sealed under vacuum in Pyrex ampules and subsequently heated to 80 °C. The $SbCl_3-GaCl_3$ mixture produces a colorless, homogeneous liquid. On the other hand, a reaction was immediately apparent in the $Ga-SbCl_3-GaCl_3$ system as the formation of a black solid phase around the gallium metal and a dark brown coloration of the upper liquid phase. After equilibration for 1 week, the liquid phase was separated by turning the ampule upside-down. Before the ampule was opened in the glovebox, excess $SbCl_3$ and $GaCl_3$ in the black solid were removed by sublimation at 80 °C.

Raman Spectroscopy. The Raman spectrum of the solidified, brown upper phase of the $Ga-SbCl_3-GaCl_3$ system was recorded after equilibration (above) on a Bruker IFS66/FRA105 FT-Raman spectrometer with a Ge-diode and a low-power Nd-YAG laser ($\lambda = 1064$ nm) providing the exciting radiation. The same principles apply to the $SbCl_3-GaCl_3$ system.

^{71}Ga and ^{121}Sb NMR Spectroscopy. The ^{121}Sb and ^{71}Ga NMR measurements were performed on a Varian Unity 300 MHz spectrometer operating at 91.456 MHz for ^{71}Ga and 72.013 MHz for ^{121}Sb.

Both naturally occurring Ga-nuclei are quadrupolar with $I = {}^3/_2$. ^{71}Ga was chosen rather than ^{69}Ga, since it has been found to be generally more easily observed due to its lower quadrupolar moment.[46] A fact with important diagnostic implications is the extremely (considering the quadrupolar nature of the Ga nuclei) sharp and narrow NMR signals from Ga(I).[47] These signals also invariably display a considerable upfield shift (>800 ppm) relative to Ga(III) signals. On the other hand, Ga(III) signals are generally broad, with the exception of highly symmetric species such as $GaCl_4^-$, whereas Ga(II) does not give any signals at all.[48] ^{71}Ga NMR may thus be used to distinguish between the different oxidation states of gallium in solution.

Elemental Analysis. Analysis of the solid phase isolated from the $3Ga-7(SbCl_3-4GaCl_3)$ system is severely complicated by the disproportionation to antimony metal and sparingly soluble oxo and oxochloro antimony compounds of varying composition which accompanies the dissolution of the substance in most solvents. However, the phase is completely soluble in *aqua regia* because of the formation of $GaCl_4^-$ and $SbCl_6^-$. Elemental analysis was therefore performed by recording ^{121}Sb and ^{71}Ga NMR spectra of the phase dissolved in *aqua regia*. The integrated peak intensities were subsequently compared with those from solutions of known Ga and Sb concentration. This method yielded consistent results for the Ga content in the phase but less reliable estimates for Sb. The complication in the latter case presumably arises because of the volatility of $SbCl_5$ and a loss of Sb during the dissolution in *aqua regia*. The ^{121}Sb NMR results were thus only semiquantitative.

Collection of Powder Diffraction Data. The powder diffraction patterns of $Bi_5(GaCl_4)_3$ and the black solid product from the $Ga-SbCl_3-GaCl_3$ system were collected with an INEL powder diffractometer, equipped with a CPS120 position sensitive detector covering 120° in 2θ and using Cu $K\alpha_1$ radiation.[49] The samples were contained in sealed 0.3 mm Lindemann capillaries and kept spinning during the 15 h of data accumulation at 295(1) K. The CPS120 detector was calibrated with a $Pb(NO_3)_2$ standard and the diffraction pattern recalculated into an equal-step ($\Delta 2\theta = 0.03056°$) pattern using a cubic-spline function.

Structural Refinements. The structure of $Bi_5(GaCl_4)_3$ was refined from the powder diffraction data by Rietveld analysis using a program which is essentially the LHPM1 program[50] modified to fit the locally used I/O formats and to use Chebyshev polynomials for background fitting. The program minimizes the quantity $\sum_i w_i(Y_{io} - Y_{ic})^2$ with $w_i = 1/Y_{io}$ and Y_{io} being the recorded intensities. Pseudo-Voigt functions with five-peak asymmetry correction[51] were used with a Lorentzian component $\gamma = \gamma_1 + \gamma_2(2\theta)$ and fwhm defined as $(U \tan^2\theta + V \tan^2\theta + W)^{1/2}$. γ_1, γ_2, U, V, W, and one asymmetry parameter were refined with peak widths limited to 18 half widths. In addition, the 2θ zero-point and fifteen background parameters (Chebyshev type I) were refined. Absorption was corrected for according to Rouse *et al.*[52] with $\mu R = 4.25$ ($\mu = 567$ cm^{-1}). Initial refinements of the data set in the range $8° \le 2\theta \le 115°$ resulted in severe profile misfit for the first reflection due to the high absorption.[53] Restricting the angular range to $11° \le 2\theta \le 115°$, and thereby excluding the first reflection, markedly improved to overall fit. The structural parameters comprised one scale factor, two unit cell parameters, and fractional coordinates and isotropic temperature factor coefficients for all atoms. The refinements were started from the parameters of $Bi_5(AlCl_4)_3$ given by Krebs *et al.*[7] The refinements were considered converged when all parameter shifts were less than 0.1 of the corresponding esd. Final residual values were $R_p = 3.9\%$, $R_{wp} = 5.2\%$, gof = 3.0, and $R_B = 2.3\%$ from 3403 step intensities, 597 Bragg reflections, and 38 refined parameters. Scattering factors for neutral atoms and anomalous scattering corrections were taken from the International Tables of X-ray Crystallography.[54]

(42) Ulvenlund, S.; Bengtsson, L. A. *J. Chem. Soc., Faraday Trans.*, in press.
(43) Fedorov, P. I.; Yakunina, V. M. *Zh. Neorg. Khim.* **1963**, *8*, 2103 (engl transl *Russ. J. Inorg. Chem.* **1963**, *8*, 1099).
(44) Fedorov, P. I.; Tsimbalist *Zh. Neorg. Khim.* **1964**, *9*, 1676 (engl transl *Russ. J. Inorg. Chem.* **1964**, *9*, 908).
(45) Corbett, J. D. *J. Am. Chem. Soc.* **1958**, *80*, 4757.
(46) Taylor, M. J. *Polyhedron* **1990**, *9*, 207.
(47) Scmidbaur, H.; Zafiropoulos, T.; Bublak, W.; Burkert, P.; Köhler, F. H. *Z. Naturforsch., A* **1986**, *41*, 315.
(48) McGarvey, B. R.; Taylor, M. J.; Tuck, D. G. *Inorg. Chem.* **1981**, *20*, 2010.
(49) Ståhl, K.; Thomasson, R. *J. Appl. Crystallogr.* **1992**, *25*, 251.
(50) Howard, C. J.; Hill, R. J. A computer program for Rietveld analysis of fixed wavelength X-ray and neutron powder diffraction patterns. Australian Atomic Energy Commission Report M112, Lucas Heights Research Laboratory, New South Wales, Australia, 1986.
(51) Howard, C. J. *J. Appl. Crystallogr.* **1982**, *15*, 615.
(52) Rouse, K. D.; Cooper, M. J.; York, E. J.; Chakera, A. *Acta Crystallogr., Sect. A* **1970**, *26*, 682.
(53) Tempest, A. *J. Appl. Crystallogr.* **1977**, *10*, 238.
(54) *International Tables for X-ray Crytallography*; Kynoch Press: Birmingham (present distributor: Kluwer Academic Publishers, Dordrecht), 1974; Vol. IV.
(55) Wadt, W. R.; Hay, P. J. *J. Chem. Phys.* **1985**, *82*, 284.

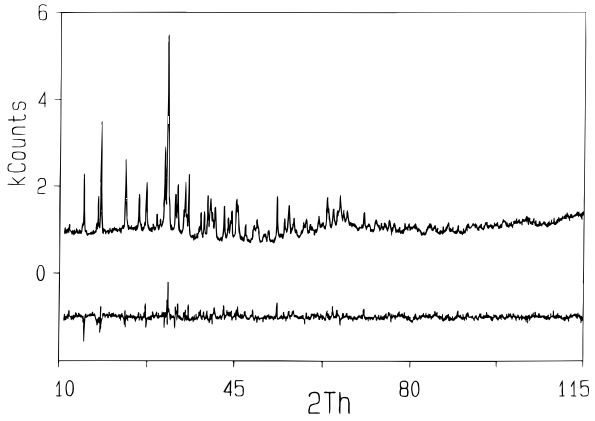

Figure 1. Diffraction pattern and final difference pattern for $Bi_5(GaCl_4)_3$.

Table 1. Fractional Coordinates ($\times 10^4$) and Isotropic Temperature Factor Coefficients for $Bi_5(GaCl_4)_3$

	x/*a*	*y*/*b*	*z*/*c*	*B* (Å^2)
Bi(1)	1618(3)	0	2500	5.6(1)
Bi(2)	0	0	3272(2)	7.1(2)
Ga	5188(7)	0	2500	3.6(2)
Cl(1)	4089(11)	26(13)	3098(4)	4.4(3)
Cl(3)	7223(11)	1696(1)	2395(4)	3.9(3)

Table 2. Comparison of the Unit Cell Parameters (Å), Distances (Å), and Angles (deg) in $Bi_5(GaCl_4)_3$ and $Bi_5(AlCl_4)_3$

		$Bi_5(GaCl_4)_3$	$Bi_5(AlCl_4)_3$
a		11.871(2)	11.860(3)
c		30.101(3)	30.100(8)
Bi(1)−Bi(1)′	× 2	3.326(6)	3.318(2)
Bi(1)−Bi(2)	× 2	3.013(5)	3.007(2)
Bi(1)′−Bi(1)−Bi(2)	× 6	56.51(7)	56.51(3)
Bi(2)′−Bi(1)−Bi(2)	× 3	100.83(17)	100.84(4)
Bi(1)′−Bi(2)−Bi(1)	× 6	66.99(14)	66.98(4)
Bi(1)−Cl(1)	× 2	3.430(12)	3.497(6)
Bi(1)−Cl(2)	× 2	3.359(11)	3.467(6)
Bi(2)−Cl(1)	× 3	3.731(13)	3.753(6)
Bi(2)−Cl(2)	× 3	3.341(12)	3.373(6)
Ga/Al−Cl(1)	× 2	2.233(12)	2.131(9)
Ga/Al−Cl(2)	× 2	2.264(12)	2.118(9)
Cl(1)−Ga/Al−Cl(1)′		107.6(7)	108.3(4)
Cl(1)−Ga/Al−Cl(2)	× 2	118.1(4)	113.7(3)
Cl(1)−Ga/Al−Cl(2)′	× 2	105.3(5)	106.4(3)
Cl(2)−Ga/Al−Cl(2)′		103.0(6)	108.5(4)

Structural parameters are given in Table 1, and the diffraction pattern and final difference pattern are shown in Figure 1.

Results and Discussion

Characterization of $Bi_5(GaCl_4)_3$. The crystal structure of $Bi_5(GaCl_4)_3$ is built from Bi_5^{3+} trigonal bipyramids and $GaCl_4^-$ tetrahedra and is isostructural with the previously characterized $Bi_5(AlCl_4)_3$.[7,18] A comparison of the unit cell parameters (Å), distances, and angles is given in Table 2. The geometry of the Bi_5^{3+} trigonal bipyramids (Figure 2) in the Ga and Al forms is identical within one σ. The significant differences between the two forms are found within the $AlCl_4^-$ and $GaCl_4^-$ anions and the intermolecular contacts. Except for the difference between the Ga−Cl and Al−Cl distances, the $GaCl_4^-$ tetrahedra (Figure 2) appear to be more distorted than the corresponding $AlCl_4^-$ tetrahedra. The generally shorter Bi−Cl distances in the $GaCl_4^-$ compound result in almost identical unit-cell parameters of the two forms, despite the longer Ga−Cl distances.

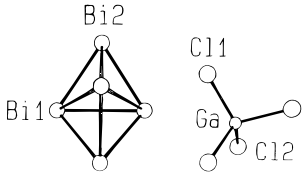

Figure 2. Labeling of the Bi_5^{3+} trigonal bipyramid and the $GaCl_4^-$ tetrahedron.

The melting point of $Bi_5(GaCl_4)_3$ was determined to be 321 °C, which is close to the corresponding value for the chloroaluminate analogue (reported to be 326 °C).[18]

The Raman scattering from $Bi_5(GaCl_4)_3$ is extremely weak due to the high absorption of the exciting radiation, and no meaningful Raman spectrum could be obtained.

Calculations on Bi_5^{3+}. The first step was to obtain the proper conditions for evaluation, *i.e.* to find an appropriate level of calculation and size of basis set. As mentioned in the Introduction, the contributions from local electron−electron correlation are expected to be small; consequently, calculations at the HF and MP2 levels are a reasonable starting point.

A more delicate task is to find good basis sets for heavy main-group systems. In the literature, there exist a number of basis sets including average relativistic effective core potentials (ARECP's not explicitly including the spin−orbit effects) which decrease the computational effort considerably. We have chosen to make a thorough study of those available, using the experimental data collected for Bi_5^{3+} as a reference to which the results of the calculations may be assessed. The results are collected and compared with experimental literature data in Table 3.

It is obvious from the results that the calculation of accurate bond distances and vibrational frequencies is far from trivial. The ARECP's of Stevens and co-workers[56] give the best results as compared to experimental data, in particular when d-type polarization functions are included (SKBJ*). The SKBJ* valence space comprises valence-sp, diffuse-sp, and d-polarization orbitals. The improvement observed when d-type functions are included in the calculations is paralleled by an *ab initio* study of E_4^{n+} (n = 0, 1, and 2; E = S, Se, and Te).[58] The inclusion of f-type and possibly g-type polarization functions could improve the results further, although previous studies have indicated that "the effects of electron correlation and a somewhat limited basis sets are mutually cancelling."[58] For polyiodide systems previously investigated, it was concluded that the reason for basis set performance most likely can be attributed to the quality and size of the valence space rather than the ARECP's.[37] This speculation is supported by the data in Table 3. However, one should remember that the use of average relativistic ARECP's in systems with high rotational symmetry, where spin−orbit effects may be substantial, may cause problems; *i.e.*, we cannot be absolutely sure that the SKBJ* basis set does well for all the right reasons. In spite of this problem, the SKBJ* basis sets are superior (as compared to our reference state: experiment), and they are therefore used throughout the rest of this work.

The optimized geometry for Bi_5^{3+}, using the SKBJ* basis set, is good at both the HF and the MP2 levels. The calculated vibrational frequencies (Table 3) decrease in the order $A_1' > A_2'' > E' > E'' > A_1' > E'$. This may be compared with the experimentally found sequence $A_1' > A_2'' > A_1' > E'' > E' >$

(56) Stevens, W. J.; Krauss, M.; Basch, H.; Jasien, P. G. *Can. J. Chem.* **1992**, *70*, 612.
(57) Ross, R. B.; Powers, J. M.; Atashroo, T.; Ermler, W. C.; LaJohn, L. A.; Christiansen, P. A. *J. Chem. Phys.* **1990**, *93*, 6654.
(58) Saethre, L.; Gropen, O. *Can. J. Chem.* **1992**, *70*, 348.

Table 3. Optimized Geometry and Vibrational Frequencies for Bi_5^{3+} Using Different Basis Sets and Methods for Calculation (D_{3h} Symmetry)[e]

				frequencies (cm^{-1})					
basis set	method	d_{eq-eq} (Å)	d_{eq-ax} (Å)	E″	E′	E′	A_2''	A_1'	A_1'
	experimental[a]	3.32	3.01	97	48	62	125	119	135
HW[b]	HF	3.474	3.095	54	52	99	124	73	123
	MP2	3.466	3.204	67	60	84	98	71	107
HW*	HF	3.318	3.003	81	64	118	149	93	150
	MP2	3.253	3.066	101	65	107	130	88	142
SKBJ[c]	HF	3.384	3.066	70	58	112	140	86	144
	MP2	3.385	3.178	83	64	95	112	79	123
SKBJ*	HF	3.328	3.012	82	64	120	151	92	154
	MP2	3.267	3.084	102	66	107	130	87	143
RPAELCI[d]	HF	3.446	3.111						
	MP2	3.355	3.171						
RPAELCI*	HF	3.488	3.130						
	MP2	3.385	3.200						
RPAELCII	HF	3.562	3.149	53	53	100	126	67	129
	MP2	3.526	3.264	64	60	86	99	69	111
RPAELCII*	HF	3.417	3.068	76	61	118	149	86	152
	MP2	3.342	3.142	95	63	105	128	82	143

[a] Experimental bond distances given as average of those in $Bi_5(AlCl_4)_3$ and $Bi_5(GaCl_4)_3$. Vibrational frequencies and assignments of $Bi_5(AlCl_4)_3$ taken from refs 7 and 8, respectively. Frequencies for Raman active modes (all except A_2'') obtained from Raman spectra of solutions of $Bi_5(AlCl_4)_3$ in molten $NaAlCl_4$ at 180 °C. IR spectra recorded from solid $Bi_5(AlCl_4)_3$ at room temperature. [b] HW are the original ECP basis sets by P. J. Hay *et al.*[55] [c] SKBJ are the ECP basis sets by W. J. Stevens *et al.*[56] [d] RPAELC*n* (n = I, II) are the ECP basis sets by R. B. Ross *et al.*[57] n = I denotes the small-size core ECP's, and n = II, the large-size ones. [e] An asterisk denotes the inclusion of d-polarization functions with an exponent of 0.17 to all basis sets in Table 3.

Table 4. Calculated and Experimental Results for the M_5^y Clusters Using SKBJ* Basis Sets

						frequencies (cm^{-1})					
cluster	method	d_{eq-eq} (Å)	d_{eq-ax} (Å)	charge ax/eq atoms	mulliken op[a] eq−ax/eq−eq	E″	E′	E′	A_2''	A_1'	A_1'
Bi_5^{3+}	experimental[b]	3.32	3.01			97	48	62	125	119	135
	HF	3.328	3.012	+0.72/+0.52	0.090/0.094	82	64	120	151	92	154
	MP2	3.267	3.084	+0.72/+0.52	0.064/0.063	102	66	107	130	87	143
	CISD	3.311	3.034	+0.72/+0.52	0.074/0.082						
Sb_5^{3+}	experimental	not available						not available			
	HF	3.151	2.849	+0.73/+0.51	0.075/0.064	120	87	170	215	135	219
	MP2	3.108	2.907	+0.73/+0.51	0.036/0.038	148	84	151	187	126	203
	CISD	3.214	2.998	+0.73/+0.51	0.057/0.056						
Pb_5^{2-}	experimental[c]	3.24	3.00					not available			
	HF	3.235	2.990	−0.33/−0.44	0.181/0.043	89	54	106	141	96	140
	MP2	3.180	3.036	−0.40/−0.40	0.069/−0.022	107	62	105	134	90	142
	CISD	3.214	2.998	−0.36/−0.42	0.132/0.024						
Sn_5^{2-}	experimental[d]	3.10	2.88					not available			
	HF	3.202	2.913	−0.32/−0.45	0.287/0.065	109	70	138	186	129	182
	MP2	3.141	2.938	−0.38/−0.41	0.159/0.039	133	74	134	176	120	184
	CISD	3.174	2.913	−0.34/−0.44	0.234/0.058						

[a] Mulliken overlap population. [b] Experimental bond distances given as average of those in $Bi_5(AlCl_4)_3$ (ref 7) and $Bi_5(GaCl_4)_3$ (this work). Vibrational frequencies and assignments of $Bi_5(AlCl_4)_3$ taken from ref 8. [c] Experimental data for (crypt-Na^+)$_2$(Pb_5^{2-}).[6] Crypt = 4,7,13,16,21,24-hexaoxa-1,10-diazabicyclo[8.8.8]hexacosane. [d] Experimental data for (crypt-Na^+)$_2$(Sn_5^{2-}).[6]

E′.[8] The calculated frequencies at the MP2 level for the highest A_1', the A_2'', and the E″ modes agree with the experimental values within 8 cm^{-1} (6%). The difference between calculated and experimental values for the remaining three modes is larger. However, the experimentally obtained vibrational spectrum consists of weak and broad peaks. There is thus a substantial uncertainty in the experimental values, especially at low wavenumbers. Furthermore, our results (*i.e.* the relative energy order of the modes) suggest that the lowest A_1' and the highest E′ modes may have been interchanged in the assignment of the experimental spectrum. Assuming that this is actually the case, the agreement between the calculated and experimental data is good, the difference now being less than 12 cm^{-1} (10%) for the four modes highest in energy. Finally, it is well-known that atom−atom distances from HF calculations often are overestimated and those obtained from MP2 calculations underestimated. For this reason, MP2 frequencies are normally too high and various scaling factors have been empirically determined for small organic molecules.[59,60] However, applying such factors in the present case would obviously be an overinterpretation of the results.

From the Mulliken overlap population values (Table 4) it is clear that Bi_5^{3+} has reasonably strong Bi−Bi bonds both equatorially and axially, **1**, and that this cluster thus is to be regarded as displaying a full three-dimensional aromaticity. This contradicts the results of previous studies using mathematical topology.[31] In these studies, deltahedral, five-membered, 12 valence electron systems were predicted *not* to display three-dimensional aromaticity (in contast to the nine-membered case). Interestingly, the Sn_5^{2-} and Pb_5^{2-} clusters conform with the topological results, as is shown and discussed below.

(59) DeFrees, D. J.; McLean, A. D. *J. Chem. Phys.* **1985**, *82*, 333.
(60) Pople, J. A.; Scott, A. P.; Wong, M. W.; Radom, L. *Isr. J. Chem.* **1993**, *33*, 345.

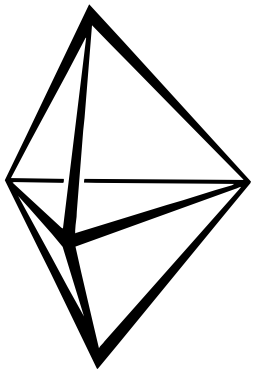

1

Bi_5^{3+} has previously been studied by eH methods,[28,29] and it is thus interesting to compare the results from these investigations with the ones reported here. The highest occupied molecular orbital (HOMO) is $3a_1'$ according to eH calculations. It mainly consists of valence 6sp-hybrid orbitals pointing equatorially away from the cluster, and it can be described as nonbonding or, alternatively, weakly bonding (the small lobes are pointing in the direction of the Bi−Bi bonds). Furthermore, it bears a strong resemblance with the stereochemically active inert-pair which often can be identified in compounds of heavier main-group elements.[39] The lowest unoccupied molecular orbitals (LUMO), 3e′, are degenerate and consist of nonbonding or weakly π-antibonding p orbitals. The HOMO's and LUMO's obtained from HF and MP2 calculations have the same general character, although they contain significant contributions from the diffuse and polarization functions, causing their symmetries to be different; the HOMO is 2e′ and the LUMO 3e′. Albeit of different symmetry, the HOMO's from eH, HF, and MP2 calculations share the property of having sp-type orbitals pointing outward from the equatorial plane of the Bi_5^{3+} cluster, **2**. Considering the character of the frontier orbitals, it is clear

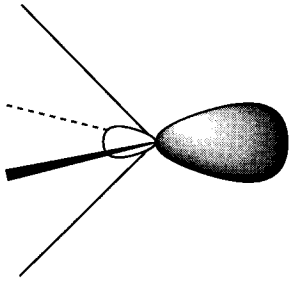

2

that the M_5^y clusters ought to be potential ligands to electrophilic transition-metal clusters stabilized by carbonyls and other π-bonding ligands, as has recently been observed in the "Zintl-metal carbonylates" such as $[Bi_4Fe_4(CO)_{13}]^{2-}$ and $[Sn_6\{Co(CO)_5\}_6]^{2-}$.[61−65]

Calculations and Synthetic Attempts on Sb_5^{3+}. The theoretical results for Sb_5^{3+} are collected in Table 4. It is clear that this cluster, which has so far evaded every synthetic attempt, must be very similar to Bi_5^{3+}. Just as for Bi_5^{3+}, the bonding scheme of Sb_5^{3+} is best described in terms of an electron-deficient aromatic system, consistent with eH results.[30] Furthermore, the total energy does not imply that Sb_5^{3+} should be expected to be less electronically stable than Bi_5^{3+}. The fact that the latter cluster can be stabilized in $GaCl_3$-based systems thus triggered an investigation of the possibility to synthesize also Sb_5^{3+} in such media, thereby taking advantage of the lower working temperature in these systems as compared to the $AlCl_3$ case.

Attempts to synthesize the hypothetical $Sb_5(GaCl_4)_3$ by directly mimicking the synthesis of $Bi_5(GaCl_4)_3$ (*i.e.* by reducing a molten $SbCl_3-4GaCl_3$ mixture by antimony metal) failed because of the low solubility of antimony metal, as have previously the attempts in the analogous $Sb-SbCl_3-AlCl_3$ system.[23,24] Only a very limited reaction could be observed as a slight yellow coloration of the liquid. However, if the stronger reducing agent gallium metal is added to molten $SbCl_3-4GaCl_3$ mixtures, an immediate reaction is observed in terms of the formation of a black solid phase (phase **I**) and a deep brown-red coloration of the liquid phase. In preliminary syntheses, a $Ga:SbCl_3$ ratio of 7:3 and an equilibration temperature of 100 °C were used, but problems with a concomitant formation of zero-valent antimony were encountered. An increase in temperature was found to lead to a complete reduction to zero-valent antimony, as was apparent from a decomposition of **I**, a loss of the color of the liquid, and a formation of antimony metal. In order to minimize the undesired formation of antimony metal, the final synthesis was performed at 80 °C using a lower $Ga:SbCl_3$ ratio of 3:7.

The final product **I** is a black, hygroscopic, porous mass, and examination under a microscope displays an apparent lack of crystalline character. The disproportionation in water and hydrochloric acid is slow and mild as compared to that of $Bi_5(GaCl_4)_3$. It decomposes to antimony metal and a volatile, colorless liquid at 213 °C. The volatile component(s) was determined to constitute 58.0 mass %, which is in reasonable agreement with the dissociation reaction (eq 1), which would give a value of 60.8 mass % volatile components.

$$Sb_5(GaCl_4)_3 \rightarrow 4Sb(s) + SbCl_3 + 3GaCl_3 \qquad (1)$$

Determination of the Ga content in phase **I** by ^{71}Ga NMR yielded a value of 17 mass % (calculated for $Sb_5(GaCl_4)_3$, 16.8%). As mentioned in the Experimental Section, the ^{121}Sb NMR results could only be used semiquantitatively as a crude estimate of the Sb content. However, the data are again compatible with the stoichiometry $Sb_5(GaCl_4)_3$. The phase slowly looses $GaCl_3$ if exposed to light. A sample exposed to light for two months was found to contain 12 mass % Ga.

The analysis of **I** must be considered with care at the present stage, since results from elemental analyses are notoriously misguiding in main-group cluster chemistry. Previous erroneous interpretations, based on elemental analyses, of totally unprecedented compounds include $Bi_5(AlCl_4)_3$[7,18] (first thought to be "$BiAlCl_4$"),[66] Bi_6Cl_7[67−69] ("BiCl"),[45] and $S_{19}(AsF_6)_2$[70] ("$S_{16}(AsF_6)_2$").[71]

(61) Schiemenz, B.; Huttner, G. *Angew. Chem.* **1993**, *105*, 295. (engl trans *Angew. Chem., Int. Ed. Engl.* **1993**, *32*, 485).
(62) Eichhorn, B. W.; Haushalter, R. C. *J. Chem. Soc., Dalton Trans.* **1990**, 937.
(63) Whitmire, K. H.; Albright, T. A.; Kang, S.-K.; Churchill, M. R.; Fettinger, J. *Inorg. Chem.* **1986**, *25*, 2799.
(64) Albright, T. A.; Yee, K. A.; Saillard, J.-Y.; Kahal, S.; Halet, J.-F.; Leigh, J. S.; Whitmire, K. H. *Inorg. Chem.* **1991**, *30*. 1179.
(65) Charles, S.; Eichhorn, B. W.; Rheingold, A. L.; Bott, S. G. *J. Am. Chem. Soc.* **1994**, *116*, 8077.
(66) Levy, H. A.; Bredig, M. A.; Danford, M. D.; Agron, P. A. *J. Phys. Chem.* **1960**, *64*, 1959.
(67) Hershaft, A.; Corbett, J. D. *J. Chem. Phys.* **1961**, *36*, 551.
(68) Hershaft, A.; Corbett, J. D. *Inorg. Chem.* **1963**, *2*, 979.
(69) Friedman, R. M.; Corbett, J. D. *Inorg. Chim. Acta* **1973**, *7*, 525.
(70) Burns, R. C.; Gillespie, R. J.; Sawyer, J. F. *Inorg. Chem.* **1980**, *19*, 1423.
(71) Gillespie, R. J.; Passmore, J. *J. Chem. Soc., Chem. Commun.* **1969**, 1333.

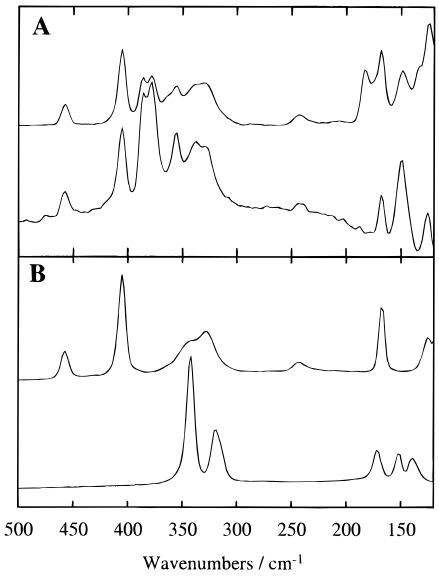

Figure 3. (**A**) Raman spectrum of a solidified sample of phase **I** dissolved in $SbCl_3-GaCl_3$ (upper spectrum) compared with that of a solidified sample of the solvent $SbCl_3-4GaCl_3$ (lower spectrum). The characteristics of these spectra may be compared with those of the spectra of solid $GaCl_3$ (B, upper spectrum) and solid $SbCl_3$ (B, lower spectrum).

Table 5. Raman Band ≤ 120 cm^{-1} Found in the Spectrum of Phase **I** dissolved in $SbCl_30GaCl_3$ at Room Temperature and Their Assignments

wavenumber (cm^{-1})	assignment	wavenumber (cm^{-1})	assignment
457, m	Ga_2Cl_6	243, w	Ga_2Cl_6
405, s	Ga_2Cl_6	183, s	Sb_n^{m+}
386, ms	$SbCl_3{\cdot}GaCl_3$	174, sh	Sb_n^{m+}
378, ms	$SbCl_3{\cdot}GaCl_3$	167, s	Ga_2Cl_6
363, sh	$Ga_nCl_{3n+1}^-$	149, s	$SbCl_3{\cdot}GaCl_3$
356, m	$SbCl_3{\cdot}GaCl_3$	133, sh	Sb_n^{m+}
337, m	Ga_2Cl_6	124, s	Ga_2Cl_6
329, m	Ga_2Cl_6		

Because of decomposition problems for phase **I** the diffraction pattern could not be indexed and consequently no cell parameters could be evaluated. No lines from Sb, $SbCl_3$, $GaCl_3$, or Ga_2Cl_4 were found. However, diffraction lines from the decomposition product $Ga(Ga_2Cl_7)$ were detected.

The Raman spectrum of **I** was impossible to record because of metallic reflection of the substance, but the Raman spectrum of a solidified sample of the upper phase of the $Ga-SbCl_3-GaCl_3$ system (*i.e.* **I** dissolved in $SbCl_3-GaCl_3$) was recorded and is displayed and compared with other relevant spectra in Figure 3 with the band positions and assignments in Table 5. The spectrum displays several low-frequency bands of high intensity which may be attributed to Sb−Sb vibrations in antimony clusters. A comparison with the calculated vibrational frequencies for Sb_5^{3+} is rendered meaningful in light of the good fit between experimental and calculated frequencies obtained for Bi_5^{3+}. Such a comparison shows that the positions of the intense, low-frequency Raman lines are in general agreement with the calculated Sb−Sb vibrations in a subvalent antimony cluster. However, the calculations are obviously not accurate enough to fulfill the diagnostic purpose as to elucidating the exact nature of the reduced antimony species formed. Two experimental spectral features are worth considering: First, none of the bands of the neat, solid solvent $SbCl_3-4GaCl_3$ are attributable to solid $SbCl_3$. On the other hand, bands attributable to Ga_2Cl_6 (which is the dominating species in solid and liquid $GaCl_3$) are present, together with four other bands which may be assigned to the structurally characterized 1:1 adduct $SbCl_3{\cdot}GaCl_3$,[72] in accordance with previous spectroscopic results.[73] According to the phase diagram of the $SbCl_3-GaCl_3$ system, $GaCl_3$ and $SbCl_3{\cdot}GaCl_3$ are the only two compounds existing in a solid $SbCl_3-4GaCl_3$ mixture.[74−76] The bands of $SbCl_3{\cdot}GaCl_3$ are found to decrease in intensity upon reduction with Ga metal, which, of course, is what should be expected if Sb(III) is reduced. Second, a shoulder at 363 cm^{-1} is found to emerge upon reduction. This shoulder corresponds to the terminal, symmetric $GaCl_3$ stretch vibrations in the chlorogallate(III) ions $Ga_nCl_{3n+1}^-$, $n = 2, 3$.[77] ^{71}Ga NMR spectra of molten samples of the liquid phase of the $Ga-SbCl_3-GaCl_3$ system at 70 °C do not reveal any Ga signals. This suggests that the gallium product formed in the oxidation of gallium metal by Sb(III) is not Ga(I), which, as mentioned in the Experimental Section, gives rise to a very sharp and narrow signal. Instead, the most likely product is Ga(III). ^{71}Ga(III) NMR signals from Ga_2Cl_6 and $Ga_nCl_{3n+1}^-$ ($n \geq 2$) are very broad or even undetectable because of the unsymmetrical magnetic environment around the gallium nuclei;[77] the same is expected to be true for $SbCl_3{\cdot}GaCl_3$. The possibility that Ga(II) is present in the liquid phase can be discarded, since the very intense symmetric Ga−Ga stretch mode at 233 cm^{-1} of the invariably Ga−Ga bonded Ga(II) chloro species[78] is not found in our spectra. Taken together, the spectral characteristics suggest that the general reaction taking place may formally be written

$$(3p - q)Ga + 3pSbCl_3{\cdot}GaCl_3 \rightarrow 3Sb_p^{q+} + 3pGaCl_3 + (3p - q)Ga^{3+} + 9pCl^- \quad (2)$$

with a concomitant formation of chlorogallate(III) ions, $Ga_nCl_{3n+1}^-$. Solidified samples of the upper phase of the $Ga-SbCl_3-GaCl_3$ system are extremely moisture sensitive and immediately turn black upon exposure to moist air. They are also very light sensitive and rapidly turn black if not protected from light. Decomposition also takes place if the intensity of the laser radiation in the Raman experiments is not kept at a sufficiently low level. In the spectra, the decomposition is evident as the gradual buildup of a low-frequency line at 174 cm^{-1} of extremely high intensity (*ca.* 10 times the intensity of the 405 cm^{-1} band of Ga_2Cl_6). As pointed out above, this sensitivity of the reduced antimony species toward radiolytic decomposition is also evident in the X-ray diffraction data of phase **I**.

To conclude, there seems to be little doubt that subvalent antimony species are formed in the $Ga-SbCl_3-GaCl_3$ system. Furthermore, the Raman characteristics suggest that Sb−Sb bonded species are present.

Calculations on Sn_5^{2-}, Pb_5^{2-}, and Tl_5^{7-}. As is obvious from the data in Table 4, the agreement with experimental structures for Sn_5^{2-} and Pb_5^{2-} is satisfactory. Unfortunately, experimental data on vibrational frequencies are unavailable. In contrast to the Sb_5^{3+}/Bi_5^{3+} pair, the bonding in Sb_5^{2-}/Pb_5^{2-} conforms to the predictions of topology (*vide supra*), and it is thus best described in terms of edge-localized M−M bonds

(72) Peylhard, C.; Potier, A. *Z. Anorg. Allg. Chem.* **1981**, *483*, 236.
(73) Chemouni, E.; Potier, E. *J. Inorg. Nucl. Chem.* **1971**, *33*, 2353.
(74) Chemouni, E.; Maglione, M.-H.; Potier, A. *Bull. Soc. Chim. Fr.* **1970**, 489.
(75) Couturier, J. C. *Rev. Chim. Miner.* **1970**, *7*, 565.
(76) Niselson, L. A.; Orshanskaya, Z. N.; Tretyakova, K. V. *Zh. Neorg. Khim.* **1974**, *19*, 1060 (engl transl *Russ. J. Inorg. Chem.* **1974**, *19*, 580).
(77) Ulvenlund, S.; Wheatley, A.; Bengtsson, L. A. *J. Chem. Soc., Dalton Trans.* **1995**, 245.
(78) Evans, C. A.; Tan, K. H.; Tapper, S. P.; Taylor, M. J. *J. Chem. Soc., Dalton Trans.* **1973**, 988.

between axial and equatorial metal atoms, **3**. Results from CISD calculations coincide well and support these ideas (Table 4).

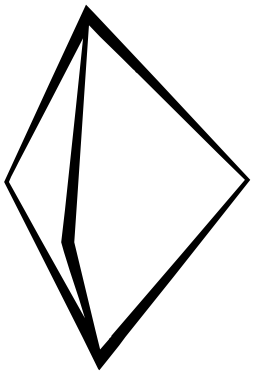

3

An analysis of the results shows that the different bonding conditions in the Sb_5^{3+}/Bi_5^{3+} (**1**) and Sn_5^{2-}/Pb_5^{2-} pairs (**3**) may be attributed to the relative energies of the valence s and p orbitals of the cluster-forming atoms. The energy gap between these orbitals is smaller in Sn and Pb than in Sb and Bi, which means that a mixing of these orbitals occurs more readily in the former case. Thus, Sn and Pb form sp orbitals (nonbonding "inert" pairs, **2**), which make the p orbitals in the equatorial plane less available for M−M bonding than for Sb and Bi.

The difference in the bonding pattern between the Sb_5^{3+}/Bi_5^{3+} and Sb_5^{2-}/Pb_5^{2-} pairs is interesting in light of the alleged impossibility to detect the Sb_5^{2-} and Pb_5^{2-} clusters in solution,[15] which contrasts starkly with the stability of Bi_5^{3+} in solution. The lack of stabilization by three-dimensional aromaticity may render five-membered tin and lead clusters thermodynamically unstable toward disproportionation to M_9^{4-} and metal according to eq 3. In solution, M_5^{2-} is thermodynamically disfavored not

$$2M_5^{2-} \rightarrow M_9^{4-} + M \qquad (3)$$

only by the aromaticity[31] of M_9^{4-} and the lack of such in M_5^{2-} but also by the lattice energy of the parent metal. In the solid state, on the other hand, the necessary coalescence of the M_5^{2-} moieties can obviously be considered hindered by large cations. By the same arguments, the corresponding disproportionation

$$2Bi_5^{3+} \rightarrow Bi_9^{5+} + Bi^{+} \qquad (4)$$

is then less likely to occur in solution, because of the lack of both the metallic lattice energy effect and the difference in aromaticity between the pentamer and the nonamer. Nevertheless, it should be noted that the stoichiometry of the characterized compound $(Bi^+)(Bi_9^{5+})(HfCl_6^{2-})_3$[79] is the same as in the hypothetical $(Bi_5^{3+})_2(HfCl_6^{2-})_3$, which has never been observed. These two alternative formulations of the total stoichiometry $Bi_{10}(HfCl_6)_3$ thus provide us with an example of the disproportionation reaction (eq 4) and show that the influence from the counterions in the solid state *in this case* favors the larger cluster ion.

(79) Friedman, R. M.; Corbett, J. D. *Inorg. Chem.* **1973**, *12*, 1134.

Table 6. Calculated Bond Distances of the M_5^y Clusters in the C_{4v} Configuration and the Energy Difference, ΔE, between C_{4v} and D_{3h} Symmetries (Positive Values Indicate D_{3h} To Be Most Stable)

cluster	method	d_{eq-eq} (Å)	d_{eq-ax} (Å)	ΔE (eV)
Bi_5^{3+}	HF	3.196	3.044	2.9780
	MP2	3.353	3.050	2.9883
Sb_5^{3+}	HF	3.017	2.868	2.8628
	MP2	3.173	2.863	3.0879
Pb_5^{2-}	HF	3.188	2.971	2.8854
	MP2	3.294	2.962	3.0399
Sn_5^{2-}	HF	3.112	2.884	2.7047
	MP2	3.210	2.860	2.8777

The theoretical calculations indicated that isolated Tl_5^{7-} ions are unstable. The reason is most probably the high charge density of this ion, and the results suggest that this ion is only stable in the solid state, where it can interact with surrounding atoms. In fact, an isolated Tl_5^{7-} would contain unbound electrons. Tl_5^{7-} may thus not be regarded as an isolated cluster in the same chemical sense as the others.

Question of Fluxionality in M_5^y Clusters. As was mentioned in the Introduction, the M_9^{4-} clusters (M = Sn or Pb) have been shown to be fluxional in solution and the same has been proposed to be true for the M_5^{2-} systems. In order to investigate this proposition, the energy difference between the D_{3h} (**1** and **3**) and C_{4v} configurations (**4**) of the M_5^y clusters

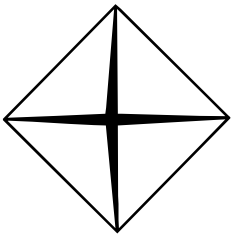

4

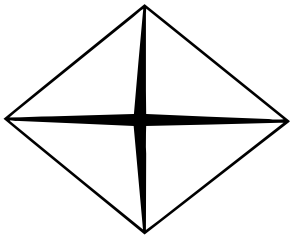

5

was calculated, including a geometry optimization within the C_{4v} point group. The results are shown in Table 6. It is clear that the energy difference between the D_{3h} and C_{4v} configurations is large in all four systems; it is on the order of 3 eV (about 300 kJ mol^{-1}). The configuration of C_{2v} symmetry (**5**, which would hypothetically be the transition state in the $D_{3h} \rightarrow C_{4v}$ rearrangement) was found to be at least 0.9 eV (about 90 kJ mol^{-1}) less stable than the D_{3h} configuration. The energy difference of about 300 kJ mol^{-1} between the D_{3h} and C_{4v} configurations clearly suggests that such a fluxional behavior of the ions is not to be expected at the temperatures normally encountered in chemical experiments.

Acknowledgment. This work has been supported by the Swedish Natural Science Research Council. The Swedish National Supercomputer Centre is acknowledged for the allocation of CPU time. Mr. Magnus Ehinger is acknowledged for his assistance in the synthesis of $Bi_5(GaCl_4)_3$.

Supporting Information Available: Figure showing powder diffraction data for phase **I** and table of reflections of $Sb_5(GaCl_4)_3$ (2 pages). Ordering information is available on any current masthead page.

IC9413981